A spectral hazy image database

Jessica Khoury, Jean-Baptiste Thomas, Alamin Mansouri

A spectral hazy image database

Jessica El Khoury[1], Jean-Baptiste Thomas[2], and Alamin Mansouri[3]

[1] ImViA Laboratory, Université Bourgogne Franche-Comté, Dijon, France
jessica.el-khoury@u-bourgogne.fr
[2] The Norwegian Colour and Visual Computing Laboratory, Norwegian University of Science and Technology (NTNU), 2815 Gjøvik, Norway

Abstract. We introduce a new database to promote visibility enhancement techniques intended for spectral image dehazing. SHIA (Spectral Hazy Image database for Assessment) is composed of two real indoor scenes M1 and M2 of 10 levels of fog each and their corresponding haze-free (ground-truth) images, taken in the visible and the near infrared ranges every $10nm$ starting from 450 to $1000nm$. Thus, the number of images that form SHIA is 1540 with a size of 1312×1082 pixels. The hazy images and the haze-free images are captured under the same illumination conditions. Three of the well-known dehazing image methods belonging to different categories were adjusted and applied on the spectral hazy images. This study confirms once again a strong dependency between dehazing methods and fog densities. It urges the design of spectral-based image dehazing able to handle simultaneously the accurate estimation of the parameters of the visibility degradation model and the limitation of artifacts and post-dehazing noise.
The database can be downloaded freely at http://chic.u-bourgogne.fr.

1 Introduction

In computer vision applications, dehazing is applied to enhance the visibility of outdoor images by reducing the undesirable effects due to scattering and absorption caused by atmospheric particles.

Dehazing is needed for human activities and in many algorithms like objects recognition, objects tracking, remote sensing [18] and sometimes in computational photography [26]. Applications that are of interest in this scope include fully autonomous vehicles typically use computer vision for land or air navigation, monitored driving [12, 30, 24] or outdoor security systems [25]. In bad visibility environments, such applications require dehazed images for a proper performance.

Image dehazing is a transdisciplinary challenge, as it requires knowledge from different fields: meteorology to model the haze, optical physics to understand how light is affected through haze and computer vision as well as image and signal processing to recover the parameters of the scene. Researchers have been always searching for an optimal method to get rid of degradation by light scattering along aerosols. Many methods have been proposed and compared to each other. Despite the large collection of methods available today, they still do not meet

efficient recovery standards and show a varying performance depending on the density of haze [8].

Earlier approaches involve multiple inputs to break down the mathematical ill-posed problem. Narasimhan *et al.* [21] calculates the haze model parameters by considering the variation of the color of pixels under different weather conditions. Feng *et al.* [11] take advantage of the deep penetration of near-infrared wavelength to unveil the details that could be completely lost in the visible band. Other ways consist in employing depth data [15] or images differently polarized [28]. Later techniques mainly focus on single image dehazing approach, which is more challenging but more suitable for the purpose of real time and costless computer vision applications. Single image dehazing was promoted through the work of He *et al.* [14], the well-known Dark Channel Prior, which gained its popularity thanks to its simple and robust real assumption based on a statistical characteristic of outdoor natural images. Therefore, numerous versions were released later, some of them propose an improvement in estimating one or more of the model's parameters and others extend the approach to other fields of application [16]. This approach, like others such as filtering based method [29], estimates explicitely transmission and airlight. Other methods overlook the physical model and improve contrast through multi-scale fusion [3], variational [13] or histogram equalization approaches [34]. Recently, like many research domains, a several machine learning approaches for image dehazing have come to light [6, 27, 17]. These models are trained on synthetic images built upon a simplistic model comparing to reality [5]. Hence the importance to build a large number of real hazy images.

To evaluate all of these various methods, some databases of hazy images are available. An early outdoor urban scene database was created on 2002, called WILD (Weather and Illumination Database) [22]. Its acquisition lasted 5 months. Thus, for one scene it contains a variety of uncontrolled weather and illumination conditions provided with scene depth and temporal data. A few years later, Tarel *et al.* [31, 30] used FRIDA and FRIDA2 as two dehazing evaluating databases dedicated to driving assistance applications. They are formed of synthetic images of urban road scenes with uniform and heterogenous layers of fog. There exist also databases of real outdoor haze-free images, for each, different weather conditions are simulated [35].

Given the significant research that has been conducted through the last decade, it turns out that synthetic images formed upon a simplified optical model do not simulate faithfully the real hazy images [7]. Therefore, several databases of real images and real fog with the groundtruth images have emerged. The real fog was produced using a fog machine. This was first used in our previous work presented in [10, 9] and it was used later by Ancuti *et al.* [4, 2] to construct a good number of outdoor and indoor real hazy images covering a large variation of surfaces and textures, and lately they introduced a similar database containing 33 pairs of dense haze images and their corresponding haze-free outdoor images [1].

The main contribution of this paper is SHIA, which is inspired from our previous color image database CHIC [10]. To the best of our knowledge, SHIA is the first database that presents for a given haze-free image, a set of spectral images with various densities of real fog. We believe that such database will promote visibility enhancement techniques for drone and remote sensing images. It will represent also a useful tool to valid future methods of spectral image dehazing. Although it contains only 2 scenes, it stands for an example to consider and to integrate efforts on a larger scale to increase the number of such complex databases.

After the description of the used material and the acquisition process of the scenes, we provide a qualitative evaluation of the three color dehazing methods that have been applied to single spectral images. Our experimental results underlines a strong dependency between the performance of dehazing image methods and the density of fog. Comparing to color images, the difference between dehazing methods is minor, since color shifting, which is usually caused by dehazing methods is not present here. The difference is mainly due to the decrease of intensity, especially induced by the physical based methods and the boost of noise.

2 Data Recording

2.1 Used material

The hyperspectral data was obtained using the Photon focus MV1-D1280I-120-CL camera based on e2v EV76C661 CMOS image sensor with 1280×1024 pixel resolution.

In order to acquire data in visible and Near-infrared (VNIR) ranges, two models of VariSpec Liquid Crystal Tunable Filters (LCTF) were used: VIS, visible-wavelength filters with a wavelength range going from 400 to 720 nm. NIR, near-infrared wavelength filter with a wavelength range going from 730 to 1100 nm. The captured VNIR images have the same size of 1312×1082 pixels and the same resolution.

Every 10 nm in the VIS range and in the NIR range, we captured a picture with a single integration time of 530 ms, which allows a sufficient light to limit the noise without producing saturated pixels over channels. This reduces as well the complexity of the preprocessing spectral calibration step (cf. Section 2.3).

In order to provide the image depth of the captured scenes, a Kinect device was used. Usually, the Kinect can detect objects up to $10m$ but it induces some inaccuracies beyond $5m$ [19]. Therefore, the camera was stand at $4.5m$ from the furthest point at the center of the scene.

To generate fog, we used the fog machine FOGBURST 1500 with the flow rate $566m^3/min$ and a spraying distance of $12m$, which emits a dense vapor that appears similar to fog. The particles of the ejected fog are water droplets whose radius is close to the radius size of the atmospheric fog $(1 - 10\mu m)$ [23].

2.2 Scenes

Scenes were set up in a closed rectangular room (length = $6.35m$, width = $6.29m$, height = $3.20m$, diagonal = $8.93m$) with a window (length = $5,54m$, height = $1.5m$), which is large enough to light up the room with daylight. The acquisition session was performed on a cloudy day to ensure an unfluctuating illumination. The objects forming the scenes were placed in front of the window, by which the sensors were placed. This layout guarantees a uniform diffusion of daylight over the objects of the scenes.

After the set up of each scene and before introducing fog, a depth image was first captured using the Kinect device, and it was then replaced by the Photon focus camera, which kept the same position through the capture of images of the fog-free scene and the foggy images at various fog densities of the same scene. The different densities of fog were generated by spreading first an opaque layer of fog, which was then evacuated progressively through the window. The same procedure was adopted for the acquisition of visible and near infrared images.

Hence, the dataset consists of two scenes, M1 and M2. The images of the scene M1 are aquired over the visible range ($450 - 720nm$) only. M2's images are captured in visible and NIR ($730 - 1000nm$) ranges. In the first set the lamp in the middle of the scene is turned off and turned on in the second. For each acquisition set, 10 levels of fog were generated besides the haze-free scene. As result, there are 308 images for M1: 11 levels (10 levels of fog + haze-free level), in each there are 28 spectral images taken at every $10nm$ from 450 to $720nm$). On the other hand, there are 1232 images for M2: on the basis of M1's images claculation, M2_VIS and M2_NIR's images are 616 each (308 for lamp on scene and 308 for lamp off scene).

2.3 Data processing

We performed a dark correction to get rid of the offset noise that appears all over the image, and a spectral calibration to deal with the spectral sensitivities of the sensor and the used filters. The dark correction consists in taking several images in the dark at the same integration time. For each pixel, we calculate the median value over these images. Therefore, we obtain the dark image. We then subtract the dark image from the spectral images taken with the same integration time. The negative values are set equal to zero [20].

For the spectral calibration, we considered the relative spectral response of the camera and the filter provided in the user manuals. For each captured image at each wavelength band with an integration time of 530 ms, we divided by the maximum peak value of the spectral response of the sensor and the corresponding filter.

3 Evaluation of dehazing techniques

The images of SHIA database have been used to evaluate three of the most representative categories of simple image dehazing approaches: DCP [14], MSCNN

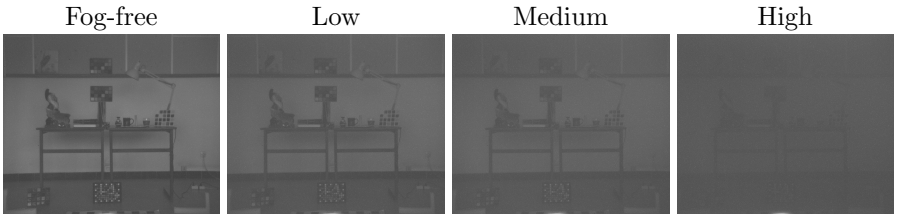

Fig. 1: **M2_VIS Lamp off**. Visible image at $550nm$ with its corresponding images taken under low, medium and high levels of fog.

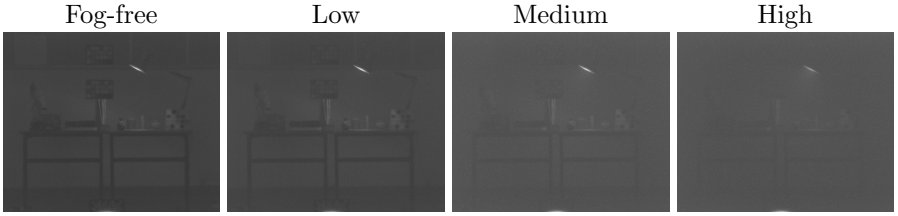

Fig. 2: **M2_NIR Lamp on**. NIR image at $850nm$ with its corresponding images taken under low, medium and high levels of fog.

[6], and CLAHE [34]. These methods have been adjusted to be applied on spectral images rather than color images. In other words, the parameters that are usually estimated through the three color bands, were estimated from the single spectral image. For the sake of readability, we have selected three levels of fog, which are denoted by low, medium and high levels (figures 1 and 2). In this article, we only display the dehazed images of the scene M2_VIS Lamp off at $550nm$ (figure 3) and the scene M2_NIR lamp on at $850nm$ (figure 4). The first row in these figures represent the foggy image at the low selected level of fog, in addition to the corresponding fog-free image and the dehazed images resulted from the three selected dehazing methods. Similarly, the second and the third rows represent the foggy image at the medium and low levels, respectively. We have calculated the scores of the classical metrics used to evaluate spectral images: PSNR, which calculate the absolute error between images; SSIM [32], which consider the neiborhood dependencies while measuring contrast and structure similarity; and MS-SSIM, which is a multiscale SSIM [33], and it performs particularly well in assessing sharpness [8]. A higher quality is indicated by a higher PSNR and closer SSIM and MS-SSIM to 1. The corresponding values are written under the images in figures 3 and 4. The average values calculated over a few selected wavelength in the VNIR range are given in table 1.

Through the visual assessment of the dehazed images presented in figures 3 and 4, we can observe that all methods, regardless their approaches and hy-

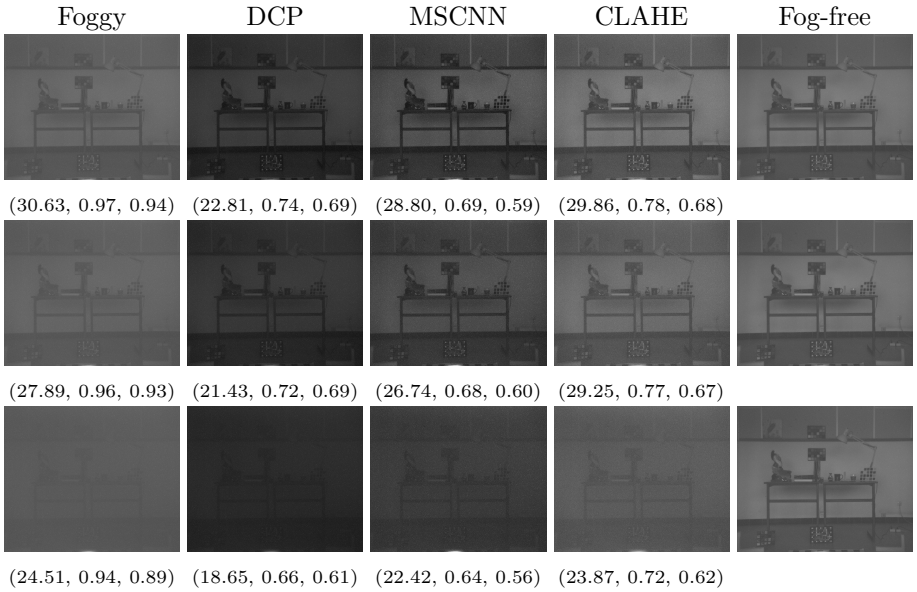

Fig. 3: **M2_VIS Lamp off taken at 550 nm**. Dehazed images processed by DCP, MSCNN and CLAHE methods, with the foggy images presented in the first column and the corresponding fog-free images in the last column. The first, second and third rows correspond to the low, medium and high levels of fog, respectively. Under each image, its corresponding scores are showed as follows: (PSNR, SSIM, MS-SSIM).

potheses, perform better at low fog densities, either at visible or near infrared range. CLAHE, which does not consider the physical model of image degradation, eliminates well the fog. However, it induces an important amount of noise that increases with the density of fog. DCP, which is a physical-based approach fails to estimate accurately the unknown parameters of the image degradation model, the airlight and the transmission of light [14]. This bad estimate produces dim dehazed images, especially at high densities of fog, where the dark channel hypothesis fails. This accords with the observation made on color images presented in our previous work [8]. MSCNN performs also an inversion of the physical model of vibility degradation. However, it estimates better the unknown parameters comparing to DCP since it is trained on a large number of hazy images. This can be deduced through its dehazed images, which are not as dark as the DCP's dehazed images are.

The metrics values provided in figures 3 and 4 have the same trends for color dehazed images across fog densities [8]. They show an increase in quality when the density of fog decreases. However, they underline a global low performance of dehazing methods. This means that haze removal is associated with secondary

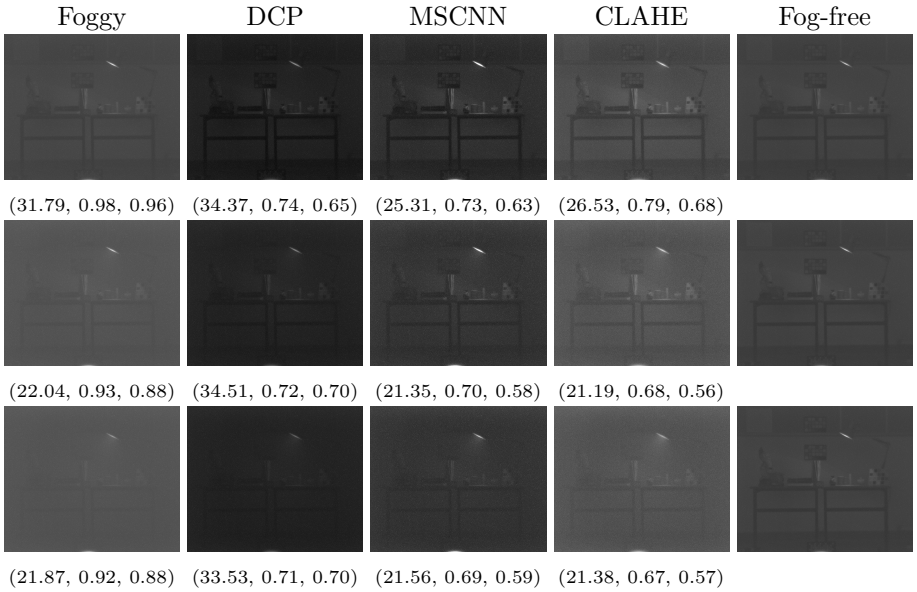

Fig. 4: **M2_NIR Lamp on taken at 850 nm**. Dehazed images processed by DCP, MSCNN and CLAHE methods, with the foggy images presented in the first column and the corresponding fog-free images in the last column. The first, second and third rows correspond to the low, medium and high levels of fog, respectively. Under each image, its corresponding scores are showed as follows: (PSNR, SSIM, MS-SSIM).

effects that restrains quality enhancement. This is likely to be handicapped by the noise and the artifacts induced in the image and the dark effect resulted from wrong estimation of visibility model parameters. These effects seem to have a severe impact on image quality more than the fog itself.

From table 1, we can conclude that:

- Foggy images are quantitatively of better quality comparing to the dehazed images, which suffer from noise, low intensity and structural artifacts.
- The scores resulted from different dehazing methods are very close to each other across wavelengths.
- The metrics values demonstrate a correlated performance between MSCNN and CLAHE over wavelengths. Although DCP has relatively higher scores, this does not mean it is the best performing method. The dimness of its resulting images seems to minimize the effect of the artifacts.

	Foggy			**DCP**			**MSCNN**			**CLAHE**		
	PSNR	SSIM	MS	PSNR	SSIM	MS	PSNR	SSIM	MS	PSNR	SSIM	MS
550 nm	26.98	0.94	0.91	22.34	0.69	0.63	24.51	0.65	0.56	25.03	0.73	0.63
650 nm	21.63	0.88	0.78	23.13	0.77	0.64	21.06	0.61	0.45	20.72	0.63	0.48
750 nm	33.23	0.97	0.95	24.03	0.69	0.66	26.07	0.70	0.63	28.10	0.70	0.66
850 nm	29.53	0.93	0.89	26.71	0.71	0.67	26.92	0.69	0.61	25.90	0.70	0.59

Table 1: The average values of PSNR, SSIM and MS-SSIM (MS) metrics calculated on the images taken under 10 densities of fog at 550, 650, 750 and 850nm

4 Conclusions

We introduce a new database to promote visibility enhancement techniques intended for spectral image dehazing. For two indoor scenes, this hard built database SHIA, contains 1540 images taken at 10 levels of fog, starting from a very light to a very opaque layer, with the corresponding fog-free images. Although the used dehazing methods are not dedicated to spectral images, they particularly introduce structural artifacts and produce noisy images. This is underlined by pixelwise quality metrics when they are compared to foggy images. Accordingly, future works should focus on reducing these effects while enhancing visibility.

Bibliography

[1] Codruta O Ancuti, Cosmin Ancuti, Mateu Sbert, and Radu Timofte. Dense haze: A benchmark for image dehazing with dense-haze and haze-free images. *arXiv preprint arXiv:1904.02904*, 2019.

[2] Codruta O Ancuti, Cosmin Ancuti, Radu Timofte, and Christophe De Vleeschouwer. O-haze: a dehazing benchmark with real hazy and haze-free outdoor images. In *Proceedings of the IEEE Conference on Computer Vision and Pattern Recognition Workshops*, pages 754–762, 2018.

[3] Codruta Orniana Ancuti and Cosmin Ancuti. Single image dehazing by multi-scale fusion. *IEEE Transactions on Image Processing*, 22(8):3271–3282, 2013.

[4] Cosmin Ancuti, Codruta O Ancuti, Radu Timofte, and Christophe De Vleeschouwer. I-haze: a dehazing benchmark with real hazy and haze-free indoor images. In *International Conference on Advanced Concepts for Intelligent Vision Systems*, pages 620–631. Springer, 2018.

[5] Alexandre Benoit, Leonel Cuevas, and Jean-Baptiste Thomas. Deep learning for dehazing: Comparison and analysis. *arXiv preprint arXiv:1806.10923*, 2018.

[6] Bolun Cai, Xiangmin Xu, Kui Jia, Chunmei Qing, and Dacheng Tao. Dehazenet: An end-to-end system for single image haze removal. *IEEE Transactions on Image Processing*, 25(11):5187–5198, 2016.

[7] Jessica El Khoury. Model and quality assessment of single image dehazing. `http://www.theses.fr/s98153`, 2016.

[8] Jessica El Khoury, Steven Le Moan, Jean-Baptiste Thomas, and Alamin Mansouri. Color and sharpness assessment of single image dehazing. *Multimedia tools and applications*, 77(12):15409–15430, 2018.

[9] Jessica El Khoury, Jean-Baptiste Thomas, and Alamin Mansouri. A color image database for haze model and dehazing methods evaluation. In *International Conference on Image and Signal Processing*, pages 109–117. Springer, 2016.

[10] Jessica El Khoury, Jean-Baptiste Thomas, and Alamin Mansouri. A database with reference for image dehazing evaluation. *Journal of Imaging Science and Technology*, 62(1):10503–1, 2018.

[11] Chen Feng, Shaojie Zhuo, Xiaopeng Zhang, Liang Shen, and Sabine Süsstrunk. Near-infrared guided color image dehazing. In *2013 IEEE International Conference on Image Processing*, pages 2363–2367. IEEE, 2013.

[12] Hasan Fleyeh and Mark Dougherty. Road and traffic sign detection and recognition. In *Proceedings of the 16th Mini-EURO Conference and 10th Meeting of EWGT*, pages 644–653, 2005.

[13] Adrian Galdran, Javier Vazquez-Corral, David Pardo, and Marcelo Bertalmio. Enhanced variational image dehazing. *SIAM Journal on Imaging Sciences*, 8(3):1519–1546, 2015.

[14] Kaiming He, Jian Sun, and Xiaoou Tang. Single image haze removal using dark channel prior. *IEEE transactions on pattern analysis and machine intelligence*, 33(12):2341–2353, 2010.

[15] Johannes Kopf, Boris Neubert, Billy Chen, Michael Cohen, Daniel Cohen-Or, Oliver Deussen, Matt Uyttendaele, and Dani Lischinski. *Deep photo: Model-based photograph enhancement and viewing*, volume 27. ACM, 2008.

[16] Sungmin Lee, Seokmin Yun, Ju-Hun Nam, Chee Sun Won, and Seung-Won Jung. A review on dark channel prior based image dehazing algorithms. *EURASIP Journal on Image and Video Processing*, 2016(1):4, 2016.

[17] Risheng Liu, Long Ma, Yiyang Wang, and Lei Zhang. Learning converged propagations with deep prior ensemble for image enhancement. *IEEE Transactions on Image Processing*, 28(3):1528–1543, 2018.

[18] Jiao Long, Zhenwei Shi, and Wei Tang. Fast haze removal for a single remote sensing image using dark channel prior. In *2012 International Conference on Computer Vision in Remote Sensing*, pages 132–135. IEEE, 2012.

[19] Kenneth David Mankoff and Tess Alethea Russo. The kinect: A low-cost, high-resolution, short-range 3d camera. *Earth Surface Processes and Landforms*, 38(9):926–936, 2013.

[20] Alamin Mansouri, FS Marzani, and Pierre Gouton. Development of a protocol for ccd calibration: application to a multispectral imaging system. *International Journal of Robotics and Automation*, 20(2):94–100, 2005.

[21] Srinivasa G Narasimhan and Shree K Nayar. Chromatic framework for vision in bad weather. In *Proceedings IEEE Conference on Computer Vision and Pattern Recognition. CVPR 2000 (Cat. No. PR00662)*, volume 1, pages 598–605. IEEE, 2000.

[22] Srinivasa G Narasimhan, Chi Wang, and Shree K Nayar. All the images of an outdoor scene. In *European conference on computer vision*, pages 148–162. Springer, 2002.

[23] Shree K Nayar and Srinivasa G Narasimhan. Vision in bad weather. In *Proceedings of the Seventh IEEE International Conference on Computer Vision*, volume 2, pages 820–827. IEEE, 1999.

[24] John P Oakley and Brenda L Satherley. Improving image quality in poor visibility conditions using a physical model for contrast degradation. *IEEE transactions on image processing*, 7(2):167–179, 1998.

[25] Niklas Pettersson. Gpu-accelerated real-time surveillance de-weathering, 2013.

[26] Ramesh Raskar. Computational photography. In *Computational Optical Sensing and Imaging*, page CTuA1. Optical Society of America, 2009.

[27] Wenqi Ren, Si Liu, Hua Zhang, Jinshan Pan, Xiaochun Cao, and Ming-Hsuan Yang. Single image dehazing via multi-scale convolutional neural networks. In *European conference on computer vision*, pages 154–169. Springer, 2016.

[28] Yoav Y Schechner, Srinivasa G Narasimhan, and Shree K Nayar. Instant dehazing of images using polarization. In *CVPR (1)*, pages 325–332, 2001.

[29] Jean-Philippe Tarel and Nicolas Hautiere. Fast visibility restoration from a single color or gray level image. In *2009 IEEE 12th International Conference on Computer Vision*, pages 2201–2208. IEEE, 2009.

[30] Jean-Philippe Tarel, Nicolas Hautiere, Laurent Caraffa, Aurélien Cord, Houssam Halmaoui, and Dominique Gruyer. Vision enhancement in homogeneous and heterogeneous fog. *IEEE Intelligent Transportation Systems Magazine*, 4(2):6–20, 2012.

[31] Jean-Philippe Tarel, Nicolas Hautiere, Aurélien Cord, Dominique Gruyer, and Houssam Halmaoui. Improved visibility of road scene images under heterogeneous fog. In *2010 IEEE Intelligent Vehicles Symposium*, pages 478–485. IEEE, 2010.

[32] Zhou Wang, Alan C Bovik, Hamid R Sheikh, and Eero P Simoncelli. Image quality assessment: from error visibility to structural similarity. *IEEE transactions on image processing*, 13(4):600–612, 2004.

[33] Zhou Wang, Eero P Simoncelli, and Alan C Bovik. Multiscale structural similarity for image quality assessment. In *The Thrity-Seventh Asilomar Conference on Signals, Systems & Computers, 2003*, volume 2, pages 1398–1402. Ieee, 2003.

[34] Zhiyuan Xu, Xiaoming Liu, and Na Ji. Fog removal from color images using contrast limited adaptive histogram equalization. In *2009 2nd International Congress on Image and Signal Processing*, pages 1–5. IEEE, 2009.

[35] Yanfu Zhang, Li Ding, and Gaurav Sharma. Hazerd: an outdoor scene dataset and benchmark for single image dehazing. In *2017 IEEE International Conference on Image Processing (ICIP)*, pages 3205–3209. IEEE, 2017.